Hydrogen Peroxide on the Surface of Europa

R. W. Carlson*, M. S. Anderson, R. E. Johnson, W. D. Smythe,
A. R. Hendrix, C. A. Barth, L. A. Soderblom, G. B. Hansen, T. B. McCord,
J. B. Dalton, R. N. Clark, J. H. Shirley, A. C. Ocampo, D. L. Matson

---

R. W. Carlson, M. S. Anderson, W. D. Smythe, A. C. Ocampo, J. H. Shirley, D. L. Matson,
Jet Propulsion Laboratory, California Institute of Technology,
Pasadena, California 91109, USA.
R. E. Johnson, Engineering Physics, University of Virginia, Charlottesville, Virginia 22903-2442, USA.
A. R. Hendrix and C. A. Barth, Laboratory for Atmospheric and Space Physics, University of Colorado, Boulder, Colorado 80309-0590, USA.
L. A. Soderblom, United Stated Geological Survey, Flagstaff, Arizona 86001, USA.
G. B. Hansen and T. B. McCord, Planetary Geosciences Division, University of Hawaii, Honolulu, Hawaii 96822, USA.
J. B. Dalton and R. N. Clark, United States Geological Survey, Denver, Colorado 80225, USA.

---

*To whom correspondence should be addressed.

Robert W. Carlson
Mail Stop 183-601
Jet Propulsion Laboratory
4800 Oak Grove Drive
Pasadena, CA 91109

Phone: 818-354-2648
Fax: 818-393-3218

E-mail: rcarlson@lively.jpl.nasa.gov

Abstract

Spatially resolved infrared and ultraviolet wavelength spectra of Europa's leading, anti-jovian quadrant observed from the Galileo spacecraft show absorption features due to hydrogen peroxide. Comparisons with laboratory measurements indicate surface H_2O_2 concentrations of about 0.13%, by number, relative to water ice. The inferred abundance is consistent with radiolytic production of H_2O_2 by intense energetic particle bombardment and demonstrates that Europa's surface chemistry is dominated by radiolysis.

The composition of a planetary surface is an important indicator of its evolution and subsequent chemical alteration. Europa's surface composition can be modified by extrusion of material from the interior (1), the infall of cometary and meteoritic material, photochemical processes, and by the deposition of material from the magnetosphere (2,3). Europa is subjected to intense bombardment by jovian magnetospheric particles – energetic electrons, protons, sulfur ions, and oxygen ions (4) – which could alter the composition through radiolysis (5,6). The relative importance of these chemical alteration processes has not been established for Europa.

Spectra of Europa indicate a water-ice surface (7) with sulfur dioxide (2,8) and hydrated minerals (9). The SO_2 could be produced by sulfate decomposition (10) or from implanted sulfur ions (2). The hydrated minerals may be evaporite salts (9), from brine extruded from a hypothetical subsurface ocean (11). Infrared (IR) spectra of Europa obtained by Galileo's near infrared mapping spectrometer (NIMS) (12) showed absorption features (13) at wavelengths of 4.25, 4.03, and 3.50 μm. Carbon dioxide and sulfur dioxide were identified (13) as the 4.25-μm and 4.03-μm absorbers, similar to previous findings for Ganymede and Callisto (14). We show here that the 3.50-μm feature, corroborated with laboratory measurements and Galileo ultraviolet spectrometer (UVS) (15) data, indicates the presence of hydrogen peroxide (H_2O_2), formed in this environment by energetic plasma irradiation of Europa's surface (6).

NIMS reflectance spectra (Fig. 1A) of Europa's leading anti-jovian quadrant (16) show characteristic features of water frost and a feature at 3.50 μm that is not due to H_2O. Hydrocarbons and ammonium-containing minerals were suggested for this feature (13), but such identifications are problematical because their absorption wavelengths do not match that observed, and both classes of compounds exhibit additional, stronger, absorption features not

evident in the NIMS spectra. For example, methanol (17) shows an absorption band at 3.53 μm and four other strong bands at 3.38, 3.35, 3.14, and 3.04-μm that are not apparent in Europa's spectrum (Fig. 1A). Similar arguments rule out other simple hydrocarbons and ammonium-bearing minerals (18). A more likely candidate for the 3.50-μm feature is H_2O_2, which produces $2\nu_2$, $\nu_2 + \nu_6$, and $2\nu_6$ combination-bending-mode absorption ($19, 20$) at $\sim$ 3.5 μm and has been predicted to occur on icy satellite surfaces (6).

For comparison to the NIMS data, we measured (21) the diffuse reflectance of H_2O_2 mixtures in water ice and found a band at 3.504 μm (Fig. 1B). Previous measurements (22) of UV-photolyzed, 10-K water ice showed the H_2O_2 feature at 3.509 μm and it shifts to 3.505 μm at 70 K. These wavelengths are consistent with the Europa feature (3.50 $\pm$0.015 μm). The widths of the Europa and laboratory feature are also consistent, both being $\sim$ 0.06 μm wide (full width at half maximum) (Fig. 1). Except for this feature, frozen aqueous H_2O_2 solutions produce near-IR spectra that are indistinguishable from those of pure water ice.

An estimate of the surface concentration of H_2O_2 is found using laboratory IR-reflectance measurements of frozen H_2O_2 – H_2O solutions at different concentrations (21). Comparing the relative band depths of these spectra with the NIMS spectrum, we find a concentration on Europa of $\sim$0.13% $\pm$ 0.07% (by number of H_2O_2 molecules, relative to H_2O; this convention is used throughout) (21). The estimate pertains to Europa's 3.5-μm wavelength, optically sensed surface layer, which is limited by water spectral absorption to depths of about the ice grain size (23), ignoring porosity. The grain size ($\sim$ 60 μm) was determined using the observed IR reflectance factor (24) and radiative transfer calculations for ice-grain surfaces (25).

Condensed H_2O_2 in Europa's surface may exist as a solid-state solution in ice, or as crystals of pure H_2O_2 or $H_2O_2 \bullet 2H_2O$ (20). However, the wavelength (3.52 μm) of the crystalline phases (at 4 and 80 K) is larger than the wavelength of Europa's feature and outside the range allowed by the estimated wavelength uncertainty. Pure amorphous H_2O_2 is precluded because its absorption band occurs at 3.56-μm (20).

Hydrogen peroxide absorbs UV radiation (26), so if our identification is correct we expect (6) a corresponding absorption signature to be present in Galileo UVS spectra (27). Disk-resolved UVS measurements (obtained concurrently with the NIMS observations) were compared to the diffuse reflectance of a frozen 0.16% solution of H_2O_2 in water (28). The spectra (Fig. 2) are consistent, both showing the onset of absorption at about 300 nm and exhibiting similar shapes at shorter wavelengths. The similarity of these spectra supports the IR identification of H_2O_2 on Europa's surface. However, numerous materials exhibit broad-band UV absorption spectra so the UV measurements alone do not provide unique identification.

The concentration used for the laboratory measurements is about the same as the Europa value, but the grain size, which also influences the reflectivity, was not determined for this laboratory sample so we cannot independently deduce H_2O_2 concentrations from these UV data. Instead, we used the IR-derived grain size and H_2O_2 UV absorption cross-sections (26, 29) to compute theoretical reflectance factor spectra (25) for various concentrations of H_2O_2. Comparing these computed reflectance factors with the Europa UV spectrum (Fig. 2) shows that the UVS observations are consistent with the IR-derived abundance for wavelengths less than 250 nm. At longer wavelengths, the observed reflectance is higher than the theoretical values; this could be

due to using 296-K, liquid-phase absorption coefficients in the calculations, which may be

inaccurate for H_2O_2 in low-temperature ice.

Production of H_2O_2 on Europa may be initiated through dissociation of surface water molecules

into H + OH by the incident energetic plasma (6). Diffusion and chemical combination of two

OH radicals yields H_2O_2. Reactive scattering of H and OH by water to form H_2O_2 also may occur

(30). The energetic particle's energy flux (31) is $\Phi \approx 5 \times 10^{10}$ keV s^{-1} cm^{-2} and each 100 eV of

energy will produce $G \approx 0.4$ H_2O_2 molecules, based on results for α-particles (32). Solar UV

radiation may also dissociate H_2O, but the average dissociating UV energy flux is <1% of that

from the energetic particles (33). With the above parameters, the production rate of H_2O_2 is $G\Phi \approx$

2×10^{11} molecules s^{-1} cm^{-2}. The incident particles can also destroy H_2O_2 molecules, either by direct

dissociation or by production of H, which then reacts with H_2O_2 (34). We estimate the rate of

destruction of H_2O_2 by the energetic particles using the flux (31) $\varphi \approx 1.2 \times 10^8$ s^{-1} cm^{-2} and an

assumed cross section of $\sigma = 1 \times 10^{-15}$ cm^2, which is the molecular size of H_2O_2. This gives a loss

rate of $\sigma\varphi \approx 1.2 \times 10^{-7}$ s^{-1}. Absorption of solar UV radiation, particularly in the 210- to 300-nm

region, dissociates H_2O_2 molecules with a diurnally averaged rate of 2.5×10^{-6} s^{-1} (gas phase

value) (33) and is effective to depths > 250 μm (23). We ignore the recombination of the

spatially contained dissociation products (the cage effect) which can reduce photon-induced loss

by a factor > 3 (35). The net loss rate will therefore be $(2.6 - 0.12) \times 10^{-6}$ s^{-1} (lifetimes ~ 4 days

and ~100 days, respectively), implying surface densities from $(0.08 - 1.7) \times 10^{18}$ cm^{-2}. The

vertical stopping distance for energetic electrons (at 60° incidence angle) is about 180 μm (31),

and less for ions, so the average H_2O_2 concentration in this ~180-μm deep radiolysis layer will be

$(0.4 - 9) \times 10^{19}$ cm^{-3}, or 0.013% to 0.3% relative to water ice. These estimated limits and our

derived concentration of 0.13% are consistent.

The abundance of H_2O_2, and the existence of a Na and O_2 atmosphere (3, 36), thought to be

produced by energetic particle bombardment of the surface (3, 10, 36), demonstrate that surface

chemistry on Europa is dominated by radiolysis. At the energy influx rates used above, the

optically-sensed surface layer can be completely modified in a few tens of years. Temporal

changes in the jovian magnetospheric energetic plasma can alter Europa's H_2O_2 abundance,

thereby changing Europa's 210- to 300-nm reflectance; such changes have been observed in

Europa's UV reflectance (37). Because CO_2 and SO_2 are present, themselves the possible

products of radiolysis (10), related products such as H_2SO_4 and various carbon compounds

should be investigated. Predictions, characterization, and identifications of surface species on

Europa must consider radiolysis effects.

REFERENCES AND NOTES

1.   R. Greeley, et al., *Icarus* **135**, 4 (1998).

2.   A. L. Lane, R. M. Nelson, D. L. Matson, *Nature* **292**, 38 (1981).

3.   M. E. Brown, R. E. Hill, *Nature* **380**, 229 (1996).

4.   W. H. Ip, D. J. Williams, R. W. McEntire, B. H. Mauk, *Geophys. Res. Lett.* **25**, 829 (1998).

5.   R. E. Johnson, *Energetic charged-particle interactions with atmospheres and surfaces* (Springer-Verlag, Berlin, 1990).

6.   R. E. Johnson, T. I. Quickenden, *J. Geophys. Res.* **102**, 10985 (1997).

7.   W. M. Calvin, R. N. Clark, R. H. Brown, J. R. Spencer, *J. Geophys. Res.* **100**, 19041 (1995).

8.   K. S. Noll, H. A. Weaver, A. M. Gonella, *J. Geophys. Res.* **100**, 19057 (1995).

9.   T. B. McCord, et al., *Science* **280**, 1242 (1998); T. B. McCord et al., *J. Geophys. Res.*, in press.

10.   R. E. Johnson, R. M. Killen, J. H. Waite, W. S. Lewis, *Geophys. Res. Lett.* **25**, 3257 (1998).

11.   M. H. Carr, et al., *Nature* **391**, 363 (1998).

12.   R. W. Carlson, et al., *Space Sci. Rev.* **60**, 457-502 (1992).

13.   W. D. Smythe, et al., Absorption bands in the spectrum of Europa detected by the Galileo NIMS instrument, XXIX Lunar and Planetary Science Conference, Houston, Texas (Lunar and Planetary Institute, 1998).

14.   R. Carlson, et al., *Science* **274**, 385 (1996); T. B. McCord et al., *Science* **278**, 271 (1997); T. B. McCord et al., *J. Geophys. Res.* **103**, 8603 (1998).

15.   C. W. Hord, et al., *Space Sci. Rev.* **60**, 503 (1992).

16.   The measurements were obtained on 6 November 1997, when Galileo was 480,000 km from Europa. The orbital phase angle and sub-solar longitude was 89° and the sub-spacecraft longitude was 152°.

17.   D. M. Hudgins, S. A. Sandford, L. J. Allamandola, A. Tielens, *Astrophys. J. Suppl.* **86**, 713 (1993).

18.   R. N. Clark, G. A. Swayze, A. Gallagher, T. V. V. King, W. M. Calvin, "The U. S. Geological Survey Digital Spectral Library: Version 1: 0.2 to 3.0 μm" *93-592* (U. S. Geological Survey, 1993).

19.   O. Bain, P. A. Giguere, *Can. J. Chem.* **33**, 527 (1955); R. L. Miller, D. F. Hornig, *J. Chem. Phys.* **34**, 265 (1961).

20.   P. A. Giguere, K. B. Harvey, *J. Mol. Spectrosc.* **3**, 36 (1959).

21.   We measured IR diffuse-reflectance spectra for frozen (~ 80 K) aqueous solutions of H_2O_2 at concentrations of 0, 0.5, 1, and 1.5%. The solution contained spectrally neutral diamond powder, producing a matte surface without specular reflection. Ice grain sizes were 5 to 15 μm. The factor relating concentration and relative band depth was found after correcting for the minor dependence of relative band depth on grain size, determined from radiative-transfer calculations (25). Grain sizes were estimated by comparing measured and computed IR reflectivities. The fractional standard error for the derived factor is 15%. We assume that the band depth is invariant with temperature; the behavior of ice bands [W. M. Grundy, B. Schmitt, *J. Geophys. Res.* **103**. 25809 (1998)] indicates that errors of ± 20% are possible. Considering other error sources, the uncertainty in the derived H_2O_2 abundance is estimated to be ± 50.

22.   P. A. Gerakines, W. A. Schutte, P. Ehrenfreund, *Astron. Astrophys.* **312**, 289 (1996).

23. We adopt, for the effective penetration depth, that level for which the optical depth for equivalent isotropic scatterers is unity. Using similarity relations [B. Hapke, *Theory of reflectance and emittance spectroscopy* (Cambridge University Press, Cambridge, 1993) p. 197] with computed single-scattering albedos and asymmetry parameters (25), we find penetration depths for a non-porous medium of 60-μm ice grains of about 60, 250, and 500 μm, for wavelengths of 3.5 μm, 210 nm, and 300 nm, respectively.

24. The reflectance factor is the ratio of the observed radiance to that of a perfectly diffuse plane reflector illuminated at the same geometry; B. Hapke (23), p. 262.

25. R. W. Carlson, T. Arakelian, *Antarctic J. U. S.* **28**, 256 (1993) outlines the computational method. We used UV and IR optical constants from S. G. Warren, *Appl. Optics* **23**, 1206 (1984) and J. E. Bertie, H. J. Labbé, E. Whalley, *J. Chem. Phys.* **50**, 4501 (1969), respectively.

26. C. L. Lin, N. K. Rohatgi, W. B. DeMore, *Geophys. Res. Lett.* **5**, 113 (1978).

27. A. R. Hendrix, C. A. Barth, C. W. Hord, A. L. Lane, *Icarus* **135**, 79 (1998).

28. Samples 3 mm thick were frozen, forming granular, diffusing surfaces. The diffuse reflectance was measured avoiding specular reflection. The UV and IR laboratory measurements were performed at the JPL Vibrational Spectroscopy Laboratory using an Analect diffuse-reflectance attachment with Biorad FTS 6000 and Cary 5E spectrometers.

29. The 3.4×10^{-4} M data from (26) was used.

30. M. T. Sieger, W. C. Simpson, T. M. Orlando, *Nature* **394**, 554 (1998).

31. We used electron and ion fluxes (for an unmagnetized body at Europa's orbit) and stopping depths in ice from J. F. Cooper, R. E. Johnson, B. H. Mauk, N. Gehrels, *Icarus* ,

in preparation. Ion fluxes were increased by a factor of two for the finite gyroradius effect

(4).

32.   M. Cottin, M. Lefort, *J. Chim. Phys.* **52**, 545 (1955). Measurements for other particles are

        needed.

33.   W. F. Huebner, J. J. Keady, S. P. Lyon, *Astrophys. Space Sci.* **195**, 1 (1992).

34.   J. A. Ghormley, A. C. Stewart, *J. Amer. Chem. Soc.* **78**, 2934 (1956).

35.   R. Schriever, M. Chergui, N. Schwentner, *J. Phys. Chem.* **95**, 6124 (1991).

36.   D. T. Hall, D. F. Strobel, P. D. Feldman, M. A. McGrath, H. A. Weaver, *Nature* **373**, 677

        (1995).

37.   D. L. Domingue, A. L. Lane, *Geophys. Res. Lett.* **25**, 4421 (1998).

38.   Portions of the work described herein were performed at the Jet Propulsion Laboratory,

        California Institute of Technology, under contract to the National Aeronautics and Space

        Administration.

Figure Captions

Fig. 1. **A.** Representative reflectance factor spectrum of Europa's leading, anti-jovian quadrant. The feature at 3.50 μm, identified as H_2O_2 absorption, is shown in the inset as the ratio to the interpolated continuum (the reflectance factor if H_2O_2 were absent). All other structure is due to water; the peak at 3.1 μm is a H_2O restrahlen feature. Detector overlap regions are evident. This spectrum is an average of nine individual spectra, covering 105° W– 125° W, 22°S - 2°N. The 3.50-μm band is found from <100° W to >140° W. **B.** Laboratory diffuse reflectance spectrum of a 0.5% frozen solution of H_2O_2 in water. Combination-bending transitions of H_2O_2 appear at 3.504 μm. No water absorption band occurs at this wavelength, as shown in the pure water ice curve (rescaled). Sample temperatures were 80 K.

Fig. 2. Europa UV reflectance factor compared to laboratory diffuse reflectance measurements and theoretical values. The Galileo UVS spectrum (filled circles) is an average for longitudes 100 ° W to 140 ° W and was obtained simultaneously with the NIMS observations. The laboratory spectra (solid lines) are for a 0.16% H_2O_2 solution and a pure water-ice sample, both at 80 K. Each was measured relative to an aluminum mirror and collectively normalized to Europa data at long wavelengths. Theoretical reflectance factors (dashed lines) were computed for the IR-derived H_2O_2 concentration (0.13% ± 0.07%) and grain size (60 μm).
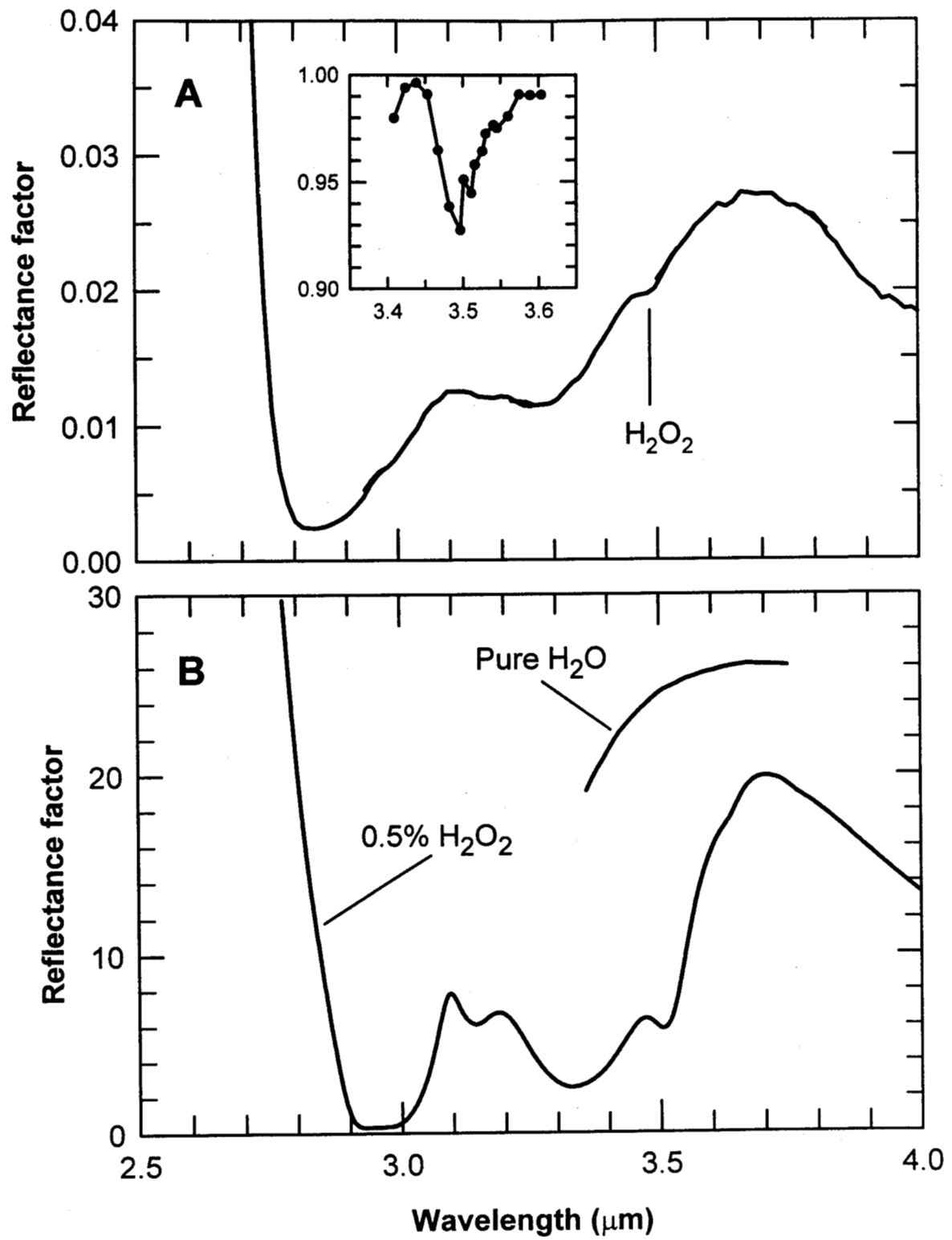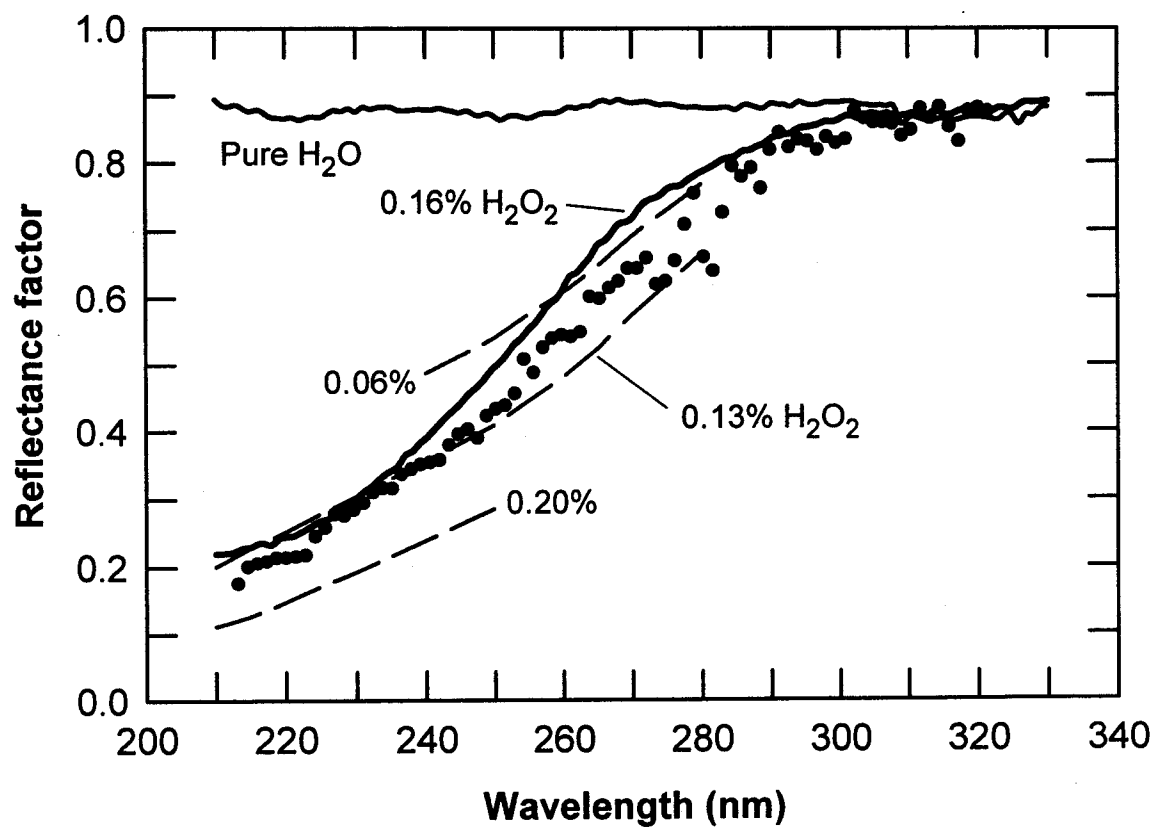
Fig. 1

Fig. 2